Carbohydrate Polymers 93 (2013) 331–338

Contents lists available at SciVerse ScienceDirect

Carbohydrate Polymers

journal homepage: www.elsevier.com/locate/carbpol

Nanoincorporation of layered double hydroxides into a miscible blend system of cellulose acetate with poly(acryloyl morpholine)

Sachi Yoshitake[a], Tetsuya Suzuki[b], Yoshiharu Miyashita[c], Dan Aoki[a], Yoshikuni Teramoto[a], Yoshiyuki Nishio[a,*]

[a] Division of Forest and Biomaterials Science, Graduate School of Agriculture, Kyoto University, Kyoto 606-8502, Japan
[b] Department of Organic and Polymer Materials Chemistry, Tokyo University of Agriculture and Technology, Koganei 184-8588, Japan
[c] Department of Chemistry and Material Engineering, Ibaraki National College of Technology, Hitachinaka 312-8508, Japan

ARTICLE INFO

Article history:
Received 15 October 2011
Received in revised form 8 March 2012
Accepted 13 March 2012
Available online 23 March 2012

Keywords:
Cellulose acetate
Miscible blends
Poly(acryloyl morpholine)
Layered double hydroxide
Nano-filler

ABSTRACT

Blend miscibility of cellulose acetate (CA) with poly(acryloyl morpholine) (PACMO) was examined by thermal transition measurements and solid-state ^{13}C NMR spectroscopy, in which CA materials of acetyl DS = 1.80–2.95 were used. All the blends prepared gave a single T_g and formed an amorphous monophase homogeneous within a distance of ~2.0 nm. An Al/Mg-based, layered double hydroxide (LDH) was modified with different ionic oligomers, and an attempt was made to incorporate the respective organophilic LDHs (3–3.5 wt%) into blend films of the miscible PACMO/CA pair, via bulk polymerization of an ACMO monomer/organo-LDH mixture and then blending CA with the polymer/inorganic hybrid precursor. Particularly, 12-hydroxystearic acid-modified LDH was well exfoliated and ultimately dispersed in the PACMO/CA matrix on a scale of less than a few tens of nanometers in thickness. This gave rise to a successful reinforcement effect leading to the improvement in thermo-mechanical property of the polymer blends.

1. Introduction

Among industrially established cellulosic products, organic ester derivatives (CEs) represented by cellulose acetate (CA) form a valuable family, gaining standard acceptance in various fields such as packaging, coating, excipients, optical films, fibers, and membranes (Edgar et al., 2001). Polymer grafting or blending can offer opportunities not only to improve the processability and original physical properties of CEs, but also to design new polymeric materials exhibiting wide-ranging properties and/or synergistic functions (Nishio, 2006). With regard to CE blends, the authors' recent efforts have been concentrated on the miscibility characterization with vinyl (co)polymers (Miyashita, Suzuki, & Nishio, 2002; Ohno, Yoshizawa, Miyashita, & Nishio, 2005; Ohno & Nishio, 2006, 2007a, 2007b) as well as with aliphatic polyesters (Kusumi, Inoue, Shirakawa, Miyashita, & Nishio, 2008). For example, CA, the most common CE, was found to be miscible with poly(*N*-vinyl pyrrolidone) (PVP) and related copolymers, in a certain range of the degree of substitution (DS) for the acetyl group. However, the number of such miscible counter-polymers for CA is still limited. In the present paper, we show another partner, poly(acryloyl morpholine) (PACMO), to form miscible blends with CA.

In the case of miscible blends of amorphous vinyl polymer/CA, attention should be drawn to the following point. Namely, viewing from the side of CA, we can improve the thermal (e.g. T_g), optical (e.g. orientation birefringence), and adsorption properties of CA, but the mechanical strength and heat resistance are often deteriorated. A remedy for such drawbacks in thermo-mechanical stability of the CA-containing physical blends is introduction of chemical cross-linkages, as has been applied to a poly(vinyl phenol)/CA system (Gaibler, Rochefort, Wilson, & Kelley, 2004). Another effective method may be the use of layered clays as nano-filler.

Since the application of organically modified montmorillonite as filler met with success to enhance performances of polyamides (Okada et al., 1990; Yano, Usuki, & Okada, 1997), a lot of attempts have been made to incorporate clays with diverse polymers including CEs (Park, Misra, Drzal, & Mohanty, 2004). The concept is, in common, to reinforce polymer matrices by exfoliation and microdispersion of layered clays. In many of the cases, the clays used were silicate ones, typically montmorillonite; they have a cation-exchanging capability and therefore the organic modifiers of the interlayer structure were usually alkyl ammonium cations. In contrast, layered double hydroxides (LDHs) form a family of lamellar inorganic compounds with exchangeable anions in the interlayer space (Newman & Jones, 1998), and they should also

* Corresponding author. Tel.: +81 75 753 6250; fax: +81 75 753 6300.
E-mail address: ynishio@kais.kyoto-u.ac.jp (Y. Nishio).

0144-8617/$ – see front matter © 2012 Elsevier Ltd. All rights reserved.
doi:10.1016/j.carbpol.2012.03.036

be a candidate for polymer-reinforcing fillers (O'Leary, O'Hare, & Seeley, 2002; Yoon, Hwang, Noh, & Lee, 2008). The anion exchange capacities are generally 2–4 times larger than the corresponding cation exchange capacity of silicate clays. Some LDHs can be easily synthesized in fine powder form, and fatty acids derived from natural lipids are also employable to replace the initial interlayer anions. Significantly, a number of hydroxyl groups are present in the surface planes of the delamination of LDHs, differing from the situation in montmorillonite.

The second objective of the present paper is to demonstrate that, if they are adequately modified and exfoliated, LDHs can act as an effective nano-filler to improve the thermo-mechanical property of miscible PACMO/CA blends.

2. Experimental

2.1. Materials

Five samples of CA, mutually different in the acetyl DS, were kindly provided from Daicel Chemical Industries, Ltd. The DS values of CAs determined by ^{1}H NMR measurements were 1.80, 2.18, 2.48, 2.70, and 2.95. The nominal, number-average molecular weights of these samples were 70,000–75,000. Acryloyl morpholine (ACMO) monomer (KOHJIN Co., Ltd.) was used after removing an inhibitor hydroquinone with an ion exchange resin DE-HIBIT 100 (Polyscience, Inc.). 2,2′-Azobisisobutyronitrile (AIBN), petroleum ether, aluminum nitrate nonahydrate ($Al(NO_3)_3{\cdot}9H_2O$), magnesium nitrate hexahydrate ($Mg(NO_3)_2{\cdot}6H_2O$), 4-aminobutyric acid (4ABA), sodium dodecyl sulfate (SDS), and 1 M NaOH aqueous solution were purchased from Nacalai Tesque, Inc. and used as received. *N*,*N*-dimethylformamide (DMF), *N*,*N*-dimethylacetamide (DMAc), chloroform ($CHCl_3$) 1,4-dioxane, 12-hydroxystearic acid (12HSA), and other reagents were purchased from Wako Pure Chemical Industries, Ltd. and used as received.

PACMO homopolymer was synthesized by radical polymerization of ACMO in $CHCl_3$. ACMO monomer was dissolved in $CHCl_3$ at a concentration of 10 wt% and AIBN was added therein at 1.0 wt% per ACMO. A flask connected with a Dimroth condenser was used for the container, and the solution was kept at 60 °C with continuous stirring under a nitrogen atmosphere. After 6 h, the solution was precipitated in an excess amount of petroleum ether, washed with the ether, and filtered. Finally, the product was dried at 50 °C for 24 h in a vacuum oven. The viscosity-average molecular weight (M_v) of the PACMO thus synthesized was evaluated as 150,000 by measuring the intrinsic viscosity ([η]) in a solvent of DMF at 25 °C; where the Mark–Houwink–Sakurada equation, $[\eta] = KM_v^{\alpha}$, was used with $K = 1.8 \times 10^{-2}$ mL g^{-1} and $\alpha = 0.65$ (Parrod & Elles, 1958).

2.2. Preparation of binary polymer blends

Binary polymer blends of PACMO/CA were prepared in film form by solution mixing and solvent evaporation. CA and PACMO solutions in DMF were separately prepared at a polymer concentration of 1.0 wt%, and aliquots of the two solutions were mixed with each other in the desired proportions. The respective mixed solutions were poured into a Teflon tray and film samples were made by solvent evaporation at 50 °C under reduced pressure (10 mmHg). The as-cast films were dried at 80 °C for 48 h in a vacuum oven. For a series of PACMO/CA (DS = 2.95) blend, DMAc was used instead of DMF, due to poor solubility of the CA (triacetate) in DMF. Virtually complete removal of these solvents from the blend samples was confirmed by FT-IR measurements (data not shown).

2.3. Preparation of LDH and organophilic LDH (LDH[M])

An Al/Mg-based LDH was obtained from a mixed solution of aluminum nitrate and magnesium nitrate by a conventional co-precipitation method (Newman & Jones, 1998). A 50 mL quantity of aqueous solution containing 0.01 mol $Al(NO_3)_3{\cdot}9H_2O$ and 0.02 mol $Mg(NO_3)_2{\cdot}6H_2O$ was slowly dropped into 200 mL of 0.05 M NaOH aqueous solution with stirring under an N_2 atmosphere at 25 °C. After regulating pH at 10 ± 0.3 with further addition of 1 M NaOH aqueous solution, the mixture was stirred vigorously for 30 min at 25 °C and then placed quiescently for 16 h at 60 °C, whereupon a solid precipitation of LDH developed.

In preparation of organophilic LDHs (LDH[M]s), a 40 mL water/ethanol mixture containing 0.02 mol organic acid as modifier (M) (ABA, SDS, or 12HSA) was slowly dropped into a 250 mL aqueous solution of $Al(NO_3)_3/Mg(NO_3)_2$ (1:2 in mol). Subsequently, the mixture was treated under the same pH and temperature conditions as in the preparation of unmodified LDH, so that a white precipitate of LDH[M] accumulated with elapsing time.

The powder products, LDH and LDH[M]s, were washed with distilled water and water/ethanol, respectively, filtered, and finally dried at 80 °C for 48 h in a vacuum oven.

2.4. Synthesis of LDH[M]–PACMO/CA nanocomposites

Bulk samples of LDH–PACMO and LDH[M]–PACMO were synthesized by radical polymerization of ACMO with ultraviolet (UV) irradiation in the presence of powdered LDH and LDH[M], respectively. AIBN (0.5 wt% per ACMO) and LDH (ca. 4.5–10 wt% per ACMO) were fed into the ACMO monomer. The radical polymerization was conducted for 2.5 h at 20 °C under a nitrogen atmosphere in a curing chamber equipped with a 10 W UV lamp FL10BLB-A (Toshiba Lighting & Technology Corporation). Subsequently, after taking off the UV lamp, the LDH– or LDH[M]–PACMO bulks were heat treated at 140 °C for 2 h under N_2-gas infusion. Residual amounts of unreacted ACMO and low-molecular-weight PACMO were washed out with ethanol. The net weight-yield of PACMO from the monomer was >95% on average. A sample of PACMO per se as reference was also synthesized in a similar manner.

The LDH– or LDH[M]–PACMO thus prepared was blended with CA in 1,4-dioxane at a total polymer concentration of 1.0 wt%, and film samples were obtained by solvent evaporation at 50 °C under normal pressure. The as-cast films of LDH–PACMO/CA and LDH[M]–PACMO/CA were dried at 80 °C for 48 h in a vacuum oven. The content of LDH or LDH[M] in the PACMO/CA matrices was adjusted ultimately to ∼3.2 wt%; for example, a bulk-polymerized PACMO containing LDH at 6.3 wt% was used for preparation of an LDH–PACMO/CA (50/50) composite having a 50:50 polymer proportion.

2.5. Measurements

Differential scanning calorimetry (DSC) was carried out with a Seiko DSC6200/EXSTAR6000 apparatus. The temperature readings were calibrated with an indium standard. The calorimetry measurements were made on ca. 5 mg samples packed in an aluminum pan at a scanning rate of 20 °C min^{-1} under a nitrogen atmosphere. Usually, the samples were first heated from 25 °C to 240 °C and subsequently quenched to −50 °C. In this first cycle, the thermal history of the respective samples was equalized to each other. Then the second scans were run from −50 to 250 °C to record stable thermograms. The glass transition temperature T_g, estimated in the second heating scan, was taken as a temperature at the midpoint of the discontinuity in heat flow. The reproducibility of the T_g data thus obtained was within ±1.5 °C. Concerning the measurements for a blend series of CA of DS = 2.95, however, the upper limit of

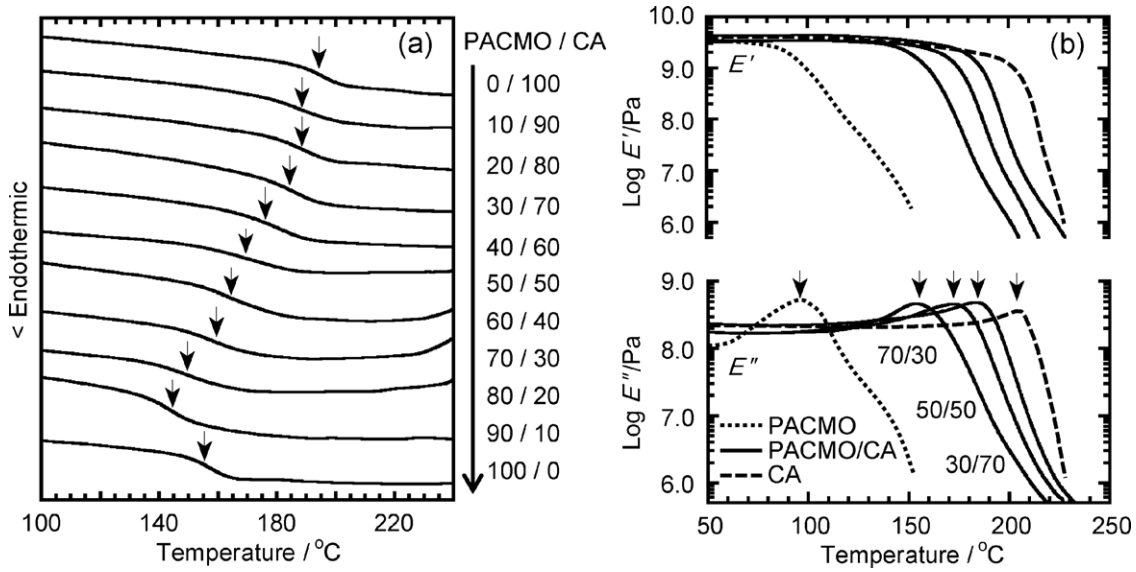

Fig. 1. (a) DSC thermograms (2nd run) and (b) DMA data obtained for PACMO/CA (DS = 2.18) blends. Positions of T_g and $T_g(E'')$ are marked by arrows in parts (a) and (b), respectively.

temperature in the heating scan was also set to be 320 °C, since a melting endotherm was expected to appear above 250 °C due to some extent of crystallinity as cellulose triacetate (Miyashita et al., 2002).

Dynamic mechanical analysis (DMA) was conducted by using a Seiko DMS6100/EXSTAR6000 apparatus. Film strips of rectangular shape (40 mm × 10 mm) were used for measurements of the temperature dependence of the dynamic storage modulus E' and loss modulus E''. Prior to the measurements, the samples were sandwiched between hard cardboards and heat treated at 160 °C for 5 min in a vacuum oven, to remove trace amounts of solvent and moisture and relax possible stresses. The measuring conditions were as follows: temperature range, 25–250 °C; scanning rate, 2 °C min^{-1}; oscillatory frequency, 10 Hz. The glass transition temperature was evaluated from the top position of an E'' peak reflecting the principal amorphous relaxation of the test sample. The data is designated as $T_g(E'')$ below, to distinguish from T_g estimated by DSC.

High-resolution solid-state NMR experiments were carried out at 20 °C with a JEOL JNM CMX-300 spectrometer operated at a ^{13}C frequency of 74.7 MHz. The magic angle spinning (MAS) rate was approximately 6 kHz. ^{13}C CP/MAS spectra were measured with a contact time of 1 ms, and a 90° pulse width of 5.0 μs was employed. In the quantifications of proton spin–lattice relaxation times in the rotating frame ($T^H_{1\rho}$) for miscible PACMO/CA blends, a contact time of 0.1 ms was used and a proton spin-locking time τ ranged from 0.25 to 24 ms. 1024 scans were conducted to obtain the ^{13}C CP/MAS spectra, while 2048 scans were accumulated for the relaxation time measurements. Chemical shifts of ^{13}C spectra represented in ppm were referred to tetramethylsilane by using the methine carbon resonance (29.5 ppm) of adamantane crystals as an external reference standard, and the spectra were essentially reproducible.

Wide-angle X-ray diffraction (XRD) measurements were made with a Rigaku RINT-2200V diffractometer at 20 °C in a reflection mode. Nickel-filtered CuKα radiation (0.1542 nm) was used at 40 kV and 30 mA. Transmission electron microscope (TEM) observations were carried out with a JEOL JEM-1220 running at an accelerating voltage of 200 kV. For the microscopic observations, composite samples were sectioned to ultrathin films (~100 nm thick) by a microtome at room temperature.

3. Results and discussion

3.1. Miscibility characterization of PACMO/CA blends

3.1.1. T_g detection by DSC and DMA

Cast films of PACMO/CA blends were mostly transparent over the whole composition range in the visual inspection, suggesting the good compatibility of the polymer pair. DSC analysis was performed for five series of PACMO/CA blends for a precise assessment of the miscibility.

Polymer–polymer miscibility is commonly estimated by determination of T_g of the blends. If any blend of a binary polymer system exhibits a single glass transition and a composition-dependent shift in T_g of the blend is observed, then the system can be regarded as a highly miscible one on the T_g-detection scale that is usually assumed to be less than a couple of tens of nanometers (Kaplan, 1976; Nishio, 1994, chap. 5; Utracki, 1990). Fig. 1a illustrates DSC thermograms obtained for a series of PACMO/CA (DS = 2.18) blends. As indicated by arrows in the figure, all the compositions of PACMO/CA = 10/90–90/10 (in weight ratio) exhibited a single T_g, roughly, increasing with an increase in the CA content, so that the system can be judged to be miscible. In Fig. 1b, DMA data for selected compositions of the PACMO/CA (DS = 2.18) series are shown for confirmation of the blend miscibility; definitely, we can see a single, principal dispersion signal shifting to the higher temperature side with increasing CA content. Some extent of discrepancy of the $T_g(E'')$ positions from the respective corresponding T_gs in DSC is observed, but this may be ascribed to the differences in the thermal history of samples as well as in the sensitivity of instrumental workings between the two measuring techniques.

Blend series of CAs having other DSs different than 2.18 also showed a single, composition-dependent T_g in the DSC measurements. Fig. 2 summarizes the T_g versus composition data for four representative PACMO/CA series including the one of DS = 2.18. Thus, PACMO was found to form a miscible blend with CA of DS = 1.80–2.95 in any mixing proportion, on the T_g-detection scale. Here it should be stressed that even the PACMO/CA (DS = 2.95) series can be a miscible system, in view of the fact that PVP was miscible with CA of DS = 2.70 but immiscible with that CA of DS = 2.95 (Miyashita et al., 2002). However, PACMO/CA (DS = 2.95) samples

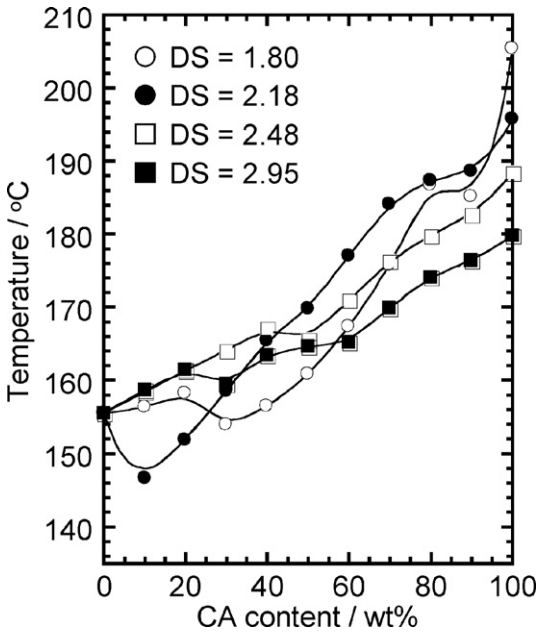

Fig. 2. Composition dependence of T_g determined by DSC for four series of PACMO/CA blends.

rich in the CA component showed a clear crystallizability as cellulose triacetate, the melting point being depressed with the mixing content of PACMO.

3.1.2. Homogeneity as estimated by ^{13}C CP/MAS NMR

To estimate the scale of homogeneity for PACMO/CA miscible blends, solid-state ^{13}C CP/MAS NMR measurements were performed. In what follows, the acetyl DS adopted for the CA component is throughout 2.18, unless otherwise specified.

Peak assignments of the spectra were made based on literature data for CA (Buchanan, Pearcy, White, & Wood, 1997; Ohno et al., 2005) and those for PACMO (Miyashita, Kimura, Suzuki, & Nishio, 1998). In the present NMR data, there was no detectable signal derived from DMF used as a solvent to prepare the blend samples. Table 1 summarizes observed values of chemical shift for the two polymer components whose structural formulae are given in Fig. 3. Both PACMO and CA possess a carbonyl carbon (—C=O), but the two resonance peaks (ca. 172–174 ppm) overlapped with each other and were hardly separated. With regard to the other carbons of PACMO (—O—CH_2—, —N—CH_2—, and —CH_2—CH—), the respective chemical shifts never showed a noticeable movement with blend composition, as can be seen in Table 1. However, the resonance signals of the pyranose and methyl carbons of the CA component (C1, C2–C5, and CH_3) moved to the side of upperfield with increasing PACMO content, by ca. 1–1.2 ppm. This implies that the intra- and/or intermolecular hydrogen-bonds in the original unblended CA might have been partly disrupted by blending with PACMO.

Table 2
$T^H_{1\rho}$ values for PACMO, CA, and PACMO/CA blends (acetyl DS = 2.18).

PACMO/CA	$T^H_{1\rho}$/ms	
	PACMO component (—CH_2—CH—)	CA component (C2–C5)
100/0	4.20	–
70/30	5.43	5.62
50/50	5.59	6.01
30/70	6.54	7.31
0/100	–	15.6

A quantitative analysis of the mixing scale in the PACMO/CA (DS = 2.18) blends was carried out through the measurements of proton spin–lattice relaxation times in the rotating frame ($T^H_{1\rho}$) established as a dynamic technique of CP/MAS NMR spectroscopy. From the $T^H_{1\rho}$ measurements, it is possible to evaluate an upper limit in heterogeneity usually on a scale of a few nanometers (McBrierty & Douglass, 1981). $T^H_{1\rho}$ values can be obtained practically by fitting the decaying carbon resonance intensity to the following single-exponential function:

$$M(\tau) = M(0)\ \exp\left(\frac{-\tau}{T^H_{1\rho}}\right) \quad (1)$$

where $M(\tau)$ is the magnetization intensity considered and τ is the spin-locking time. In a binary polymer blend, if the two constituent polymers are mixed closely enough to allow a cooperative spin-diffusion, the $T^H_{1\rho}$ values for different protons belonging to the respective components may be equalized to each other (Masson & Manley, 1991a, 1991b).

Fig. 3 illustrates the decay behavior of ^{13}C resonance for PACMO, CA (DS = 2.18), and their 50/50 blend. The resonance peak of pyranose C2–C5 carbons (ca. 74 ppm) of CA and that of —CH_2—CH— carbons (ca. 37 ppm) of PACMO were monitored in this experiment. The slope of each semi-logarithmic plot gives a $T^H_{1\rho}$ value as the time constant of the relaxation process.

Table 2 lists $T^H_{1\rho}$ data thus estimated for PACMO, CA (DS = 2.18), and their blends with 70/30–30/70 compositions. The relaxation times quantified for the unblended PACMO and CA samples were 4.2 ms and 15.6 ms, respectively. In their blends, the $T^H_{1\rho}$ value of the PACMO component rises appreciably with increasing CA content, while that of the CA component diminishes rather quickly with increasing PACMO content. Consequently, the two $T^H_{1\rho}$ values at each composition almost coincide with each other. Taking account of some tolerance in the relaxation measurements, it is reasonable to assume that the two polymer components in the blends are coexistent within a range where the mutual ^1H-spin diffusion is permitted over a period of the homogenized $T^H_{1\rho}$, e.g. 5.8 ms on average for the 50/50 composition of PACMO/CA.

An effective path length L of the spin diffusion in a time ($T^H_{1\rho}$) is given by the following equation (McBrierty & Douglass, 1981):

$$L \cong (6DT^H_{1\rho})^{1/2} \quad (2)$$

Table 1
^{13}C chemical shifts of PACMO, CA, and PACMO/CA blends (acetyl DS = 2.18).

PACMO/CA	^{13}C chemical shifts/ppm								
	PACMO component				CA component				
	—C=O	—O—CH_2—	—N–CH_2—	—CH_2—CH—	C1	C2–C5	C6	—C=O	—CH_3
100/0	174.2	67.7	46.8/43.3	37.1	–	–	–	–	–
70/30	173.6	67.5	46.7/43.3	37.0	101.7	73.0	–	173.6	20.9
50/50	172.4	67.4	46.3/43.0	37.0	102.0	73.3	–	172.4	21.1
30/70	172.0	68.0	46.4/42.9	37.3	102.3	74.3	–	172.0	21.4
0/100	–	–	–	–	102.7	74.5	63.7	171.6	21.7

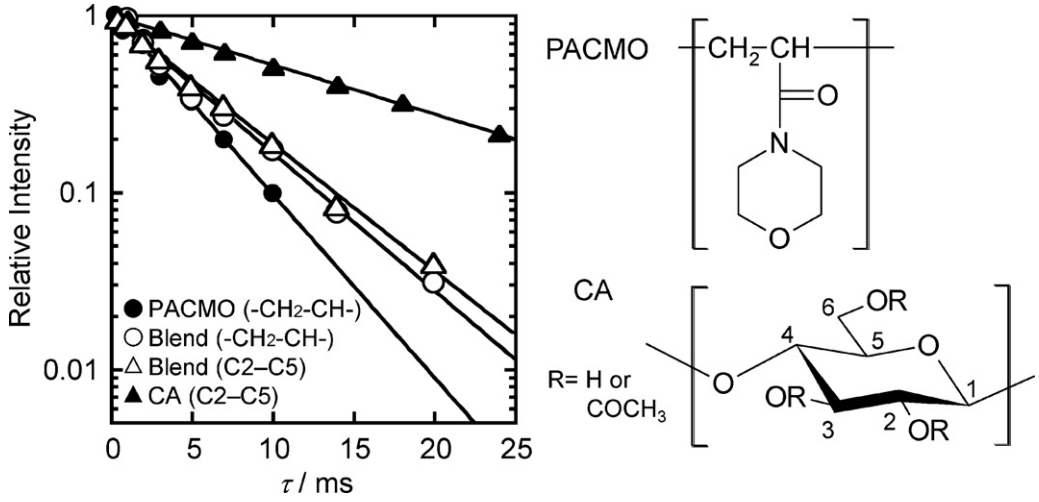

Fig. 3. Semilogarithmic plots of the decay of ^{13}C resonance intensities as a function of spin-locking time τ, for film samples of PACMO, CA (DS = 2.18), and their 50/50 blend. The resonance peak of pyranose C2–C5 carbons of CA and that of —CH_2—CH— carbons of PACMO were monitored.

where D is the diffusion coefficient, usually taken to be $\sim 1.0 \times 10^{-16}\ m^2\ s^{-1}$ in organic polymer materials (Assink, 1978; Radloff, Boeffel, & Spiess, 1996; Spiegel, Schmidt-Rohr, Boeffel, & Spiess, 1993; Zhang, Takegoshi, & Hikichi, 1992). With $T_{1\rho}^{H}$ values of 5.4–7.3 ms obtained for the PACMO/CA blends, the diffusion path length can be calculated as $L = 1.8$–2.1 nm. Accordingly, it is assured that the relevant blends are homogeneous on a few nanometers scale.

3.2. Nano-architecture and thermo-mechanical property of LDH[M]–PACMO/CA composites

3.2.1. Dispersibility of LDH[M] as filler

LDH (Al/Mg = 1/2) was prepared from a mixed solution of aluminum nitrate and magnesium nitrate by the co-precipitation method described in Section 2. Organically modified LDHs, LDH[M]s, were obtained by exchanging NO_3^- of LDH with anionic oligomers, 4ABA, SDS, and 12HSA. XRD measurements were carried out to evaluate the interlayer spacing of the three LDH[M]s in the respective original produced forms, and also to see the possible space change following their incorporations into PACMO and PACMO/CA (DS = 2.18) matrices. Selected data of the collected XRD intensity profiles are displayed in Fig. 4.

As shown uppermost in Fig. 4a, the unmodified LDH exhibited a strong diffraction at $2\theta = 11.5^\circ$ to yield a d-spacing of 0.772 nm, which corresponds to the basal plane distance d_{001} (Cavani, Trifirò, & Vaccari, 1991; Whilton, Vickers, & Mann, 1997). Other peaks observed at $2\theta = 23.2^\circ$ and 34.8° correspond to the secondary (0 0 2) and tertiary (0 0 3) diffractions, respectively, so that we can confirm the successful synthesis of LDH as an objective one. After the organic modification, the spacing d_{001} increased apparently with an elongation in chain length of the intercalated anionic oligomer; i.e., $d_{001} = 0.866$ nm ($2\theta = 10.2^\circ$) for LDH[4ABA], 3.29 nm ($2\theta = 2.68^\circ$) for LDH[SDS], and 3.65 nm ($2\theta = 2.42^\circ$) for LDH[12HSA], each evaluated from the corresponding XRD profile. It is thus assured that the interlayer spacing of these LDH[M]s is expanded relative to that of the original LDH; however, the alkyl chains would be inclined, more or less, to the basal plane.

Next, we examined the exfoliation and dispersibility of LDH[M]s in polymer matrices. Fig. 4 includes XRD data

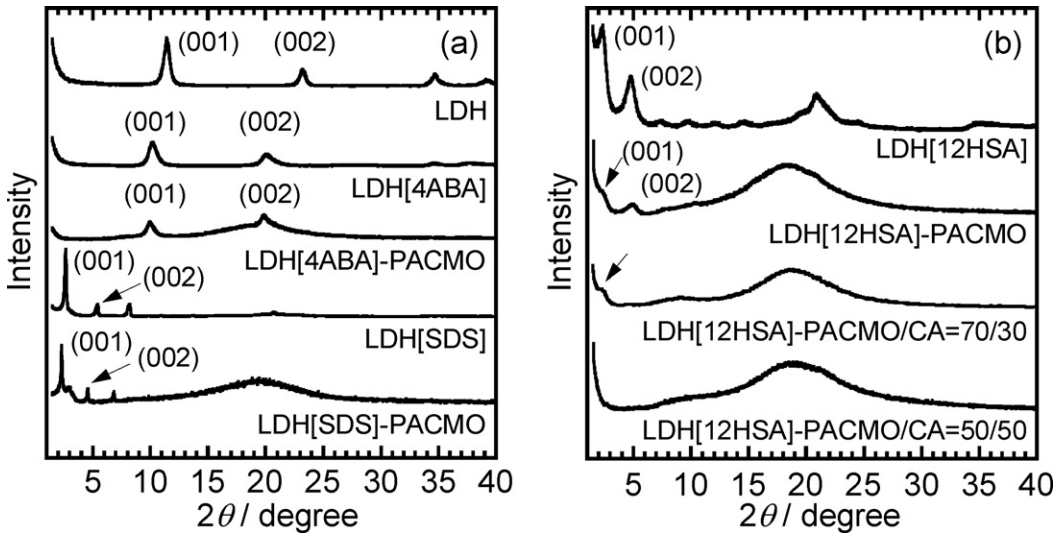

Fig. 4. XRD profiles of LDH[M]s, measured before and after hybridizing with PACMO and PACMO/CA blends: (a) data for LDH (unmodified), LDH[4ABA], LDH[4ABA]–PACMO, LDH[SDS], and LDH[SDS]–PACMO; (b) data for LDH[12HSA], LDH[12HSA]–PACMO, and 70/30 and 50/50 compositions of LDH[12HSA]–PACMO/CA. The content of LDH[M] is 6.3 wt% in all the LDH[M]–PACMO samples and ~3.2 wt% in the LDH[12HSA]–PACMO/CA composites.

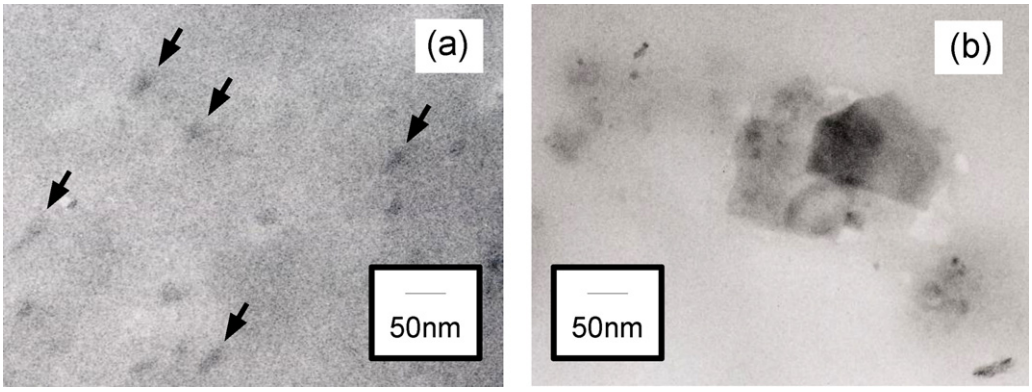

Fig. 5. TEM micrographs obtained for a LDH[12HSA]–PACMO/CA composite (polymer composition, 50/50; LDH[12HSA] content, 3.15 wt%).

measured for LDH[M]–PACMO precursor samples (see Section 2) and LDH[12HSA]–PACMO/CA composites of 70/30 and 50/50 in polymer composition. Regarding the precursor samples, any of the added LDH[M]s provided the (0 0 1) and (0 0 2) diffractions at almost the same angular positions as those taken in the unincorporated state; but, the diffraction peaks obtained for LDH[12HSA]–PACMO were generally blunt. As to LDH[12HSA]–PACMO/CA composites, the primary (0 0 1) diffraction of LDH[12HSA] was still observable for PACMO-rich compositions (≥70 wt% PACMO), whereas, for polymer compositions containing 50 wt% and more CA, we found no signal reflecting such a stacked lamellar structure of LDH[12HSA] (see Fig. 4b). From this result, it is presumed that exfoliation of LDH[12HSA] is promoted by blending with CA, possibly due to some interaction between CA and the organo-LDH having a hydroxyl group. In the case where LDH[SDS] was hybridized with PACMO/CA blends, the layered structure was barely retained in the 50/50 polymer matrix and ultimately disappeared at the 30/70 composition (data not shown). When the disperser was LDH[4ABA], both the primary and secondary diffraction peaks characteristic of the layered structure were clearly observed for the hybrid even with the composition of PACMO/CA = 50/50. This situation was also applicable to the unmodified LDH used similarly. Based on these observations, the extent of delamination and therefore the dispersibility, too, of the LDH[M] series in the miscible PACMO/CA system may be ranked as follows: unmodified LDH ≈ LDH[4ABA] < LDH[SDS] < LDH[12HSA].

The higher dispersibility of LDH[12HSA] in the composites with PACMO/CA (CA ≥ 50 wt%) was also supported by TEM observations. A major morphological data is shown in Fig. 5a; it is observed that LDH[12HSA] are dispersed on a scale of less than a few tens of nanometers (in thickness) in a 50/50 PACMO/CA matrix. Fig. 5b represents a rare observation; we can see the front faces of somewhat larger lamellar fragments of LDH[12HSA] partly overlapping with each other.

3.2.2. Enhancement of thermo-mechanical performance

In order to estimate the reinforcement effect of LDH[M]s as filler in the PACMO/CA system, DMA measurements were performed and the data were compared between the presence and absence of the filler, and between three incorporations mutually

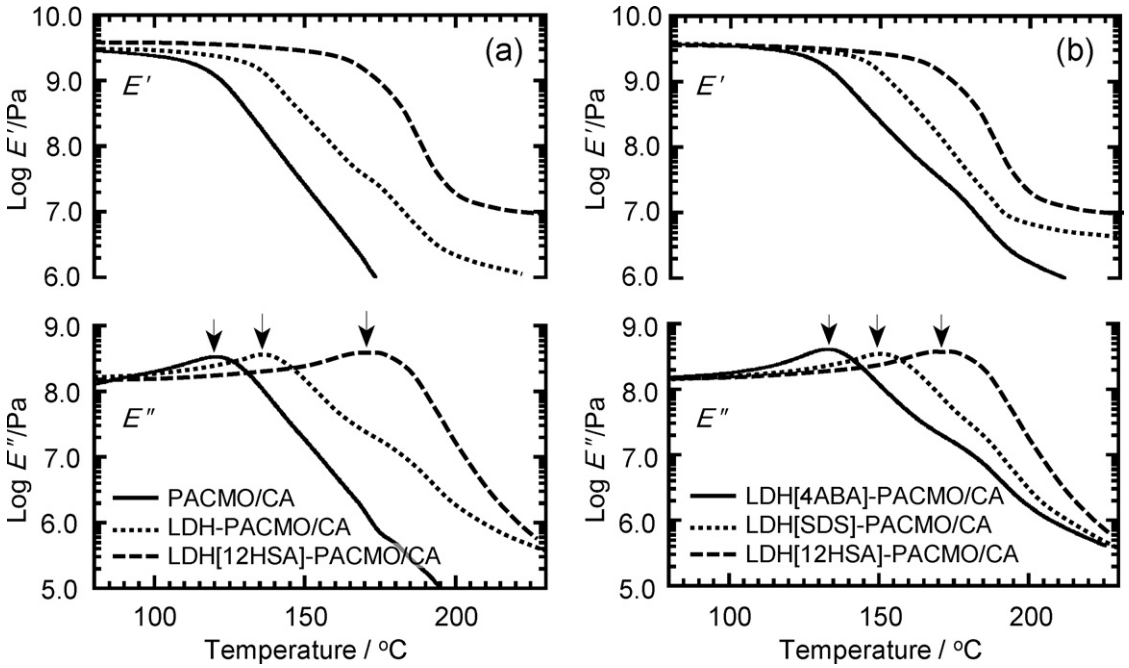

Fig. 6. Temperature dependence of E' and E'': (a) data for PACMO/CA (—), LDH–PACMO/CA (···), and LDH[12HSA]–PACMO/CA (– – –); (b) data for LDH[4ABA]–PACMO/CA (—), LDH[SDS]–PACMO/CA (···), and LDH[12HSA]–PACMO/CA (– – –). Their polymer compositions were unified as PACMO/CA = 50/50, and the content of LDH or LDH[M] was adjusted to ~3.2 wt%. Arrows indicate a $T_g(E'')$ position.

different in the organic modifier of LDH as well. The polymer composition of the respective samples used was fixed as PACMO/CA (DS = 2.18) = 50/50. Fig. 6 collects the DMA results to be compared.

Looking at the data for a 50/50 polymer blend as a reference sample without any clay (Fig. 6a), we can see a rapid and intense fall of the modulus E' in the glass transition region. This blend sample was obtained via the same procedures (including bulk-polymerization of ACMO) as adopted for the composite preparation, and $T_g(E'') = 121\,^\circ$C was read off from the E''-peak position. Following the onset of the glass transition on heating, the micro-Brownian motions of the intimately mixed two polymers appear to be more and more enhanced with increasing temperature, and above ~190 °C the values of both E' and E'' were almost out of the measurement range, due to the occurrence of plastic flow of the film specimen.

With the incorporations of LDH and LDH[M]s into the polymer blend, there occurred a definite shift in $T_g(E'')$ toward the higher temperature side. The unmodified LDH filler gave rise to a moderate elevation in $T_g(E'')$ by 10–15 °C relative to that (121 °C) of the plain PACMO/CA blend, as well as some extent of suppression in the plastic flow of the polymer matrix, as exemplified by a DMA data in Fig. 6a for the corresponding LDH–PACMO/CA composite. When LDH[12HSA] was used as the filler, a more drastic suppression of the E'-drop accompanying the glass transition took place, attended by a clear plateau region, as imparted by an E' versus temperature plot in Fig. 6a for the composite concerned. In the corresponding E'' data, an upward shift in the peak temperature was also more conspicuous ($T_g(E'') = 169\,^\circ$C), compared with that observed for the incorporation of unmodified LDH. It is thus found that the dispersing agent LDH[12HSA] serves as a highly effective reinforcer for the miscible polymer blend to improve the thermo-mechanical property.

In Fig. 6b, DMA data obtained for the incorporations of LDH[4ABA] and LDH[SDS] are compared with that for the case using of LDH[12HSA]. As is apparent there, the LDH[SDS] filler also led to a considerable shift in the E'' peak of the composite concerened ($T_g(E'') = 149\,^\circ$C), together with prevention of a sweeping drop of the modulus E' in the temperature range of $>T_g(E'')$. However, the reinforcement effect is reasonably taken as being inferior to the corresponding one of LDH[12HSA]. In the employment of LDH[4ABA], the organic modifier having a shorter alkyl chain and a potentially cationic amino-group, the composite synthesized provided a DMA data similar to that for the LDH–PACMO/CA sample (shown in Fig. 6a).

By the comparative DMA investigation described above, we can rank the effectiveness of LDH and LDH[M]s in reinforcing the thermo-mechanical property of PACMO/CA blends, as follows: unmodified LDH ≈ LDH[4ABA] < LDH[SDS] < LDH[12HSA]. This rank order is in accordance with that estimated in advance as to the dispersibility of the fillers in the polymer blend matrices. In relation to the highest effectiveness of LDH[12HSA], a complementary DMA measurement was made on a LDH[SA]–PACMO/CA composite, the organic modifier of LDH being just stearic acid (SA). The extent of the reinforcing effect of LDH[SA] was much lower than that of LDH[12HSA] and even inferior to that of LDH[SDS]. It may be suggested that a hydroxyl side-group on the alkyl chain of 12HSA (derived from caster oil) plays an important role, to act as a kind of cross-linking site of the layered clay with the CA component of the polymer blend.

4. Conclusions

Blends of PACMO/CA (DS = 1.80–2.95) pairs are miscible, which was proved by the detection of a single T_g varying with composition in DSC and DMA measurements. The homogeneity scale in the miscible amorphous blends may be taken to be within the limits of ~2.0 nm, as was exemplified by the $T_{1\rho}^{H}$ quantifications in solid-state ^{13}C NMR measurements.

An Al/Mg-based LDH and three organophilic LDHs (LDH[M]s) were used as filler to improve the thermo-mechanical property of the miscible PACMO/CA blend material. The fillers were incorporated at a concentration of 3–3.5 wt% by solution blending of CA with an LDH[M]–PACMO precursor prepared by bulk polymerization of ACMO containing the LDH[M] powder. The reinforcement effect of the respective filler incorporations was assessed by DMA for the objective LDH[M]–PACMO/CA composite, from the extent of suppression in an E' drop appearing in the glass transition temperature region as well as from that of elevation in $T_g(E'')$. As a consequence, we found a rank order, unmodified LDH ≈ LDH[4ABA] < LDH[SDS] < LDH[12HSA], regarding the effectiveness as reinforcer. This order agreed with that for the dispersibility of the fillers in the PACMO/CA medium; the latter was estimated by XRD and TEM measurements. Especially the LDH modified with 12HSA was better exfoliated and ultimately dispersed in the blend matrix on a scale of less than a few tens of nanometers in thickness, giving rise to the highest reinforcement effect in this series of LDH[M].

Beyond the present successful example, adequately modified LDHs would be widely available for the improvement in physical and/or physicochemical properties of various compositional materials based on cellulosics or other polysaccharides, by using an incorporation procedure suitable for each individual case of the compositions.

Acknowledgments

We acknowledge Prof. K. Takabe of Kyoto University for having afforded the TEM measurement facilities. This work was partially financed by a Grant-in-Aid for Scientific Research (A) (No. 23248026 to YN) from the Japan Society for the Promotion of Science.

References

Assink, R. A. (1978). Nuclear spin diffusion between polyurethane microphases. *Macromolecules*, *11*, 1233–1237.

Buchanan, C. M., Pearcy, B. G., White, A. W., & Wood, M. D. (1997). The relationship between blend miscibility and biodegradation of cellulose acetate and poly(ethylene succinate) blends. *Journal of Environmental Polymer Degradation*, *5*, 209–223.

Cavani, F., Trifirò, F., & Vaccari, A. (1991). Hydrotalcite-type anionic clays: Preparation, properties and applications. *Catalysis Today*, *11*, 173–301.

Edgar, K. J., Buchanan, C. M., Debenham, J. S., Rundquist, P. A., Seiler, B. D., Shelton, M. C., et al. (2001). Advances in cellulose ester performance and application. *Progress in Polymer Science*, *26*, 1605–1688.

Gaibler, D. W., Rochefort, W. E., Wilson, J. B., & Kelley, S. S. (2004). Blends of cellulose ester/phenolic polymers – chemical and thermal properties of blends with polyvinyl phenol. *Cellulose*, *11*, 225–237.

Kaplan, D. S. (1976). Structure-property relationships in copolymers to composites: Molecular interpretation of the glass transition phenomenon. *Journal of Applied Polymer Science*, *20*, 2615–2629.

Kusumi, R., Inoue, Y., Shirakawa, M., Miyashita, Y., & Nishio, Y. (2008). Cellulose alkyl ester/poly(ε-caprolactone) blends: Characterization of miscibility and crystallization behaviour. *Cellulose*, *15*, 1–16.

Masson, J.-F., & Manley, R. St. J. (1991a). Cellulose/poly(4-vinylpyridine) blends. *Macromolecules*, *24*, 5914–5921.

Masson, J.-F., & Manley, R. St. J. (1991b). Miscible blends of cellulose and poly(vinylpyrrolidone). *Macromolecules*, *24*, 6670–6679.

McBrierty, V. J., & Douglass, D. C. (1981). Recent advances in the NMR of solid polymers. *Journal of Polymer Science Macromolecular Reviews*, *16*, 295–366.

Miyashita, Y., Kimura, N., Suzuki, H., & Nishio, Y. (1998). Cellulose/poly(acryloyl morpholine) composites: Synthesis by solution coagulation/bulk polymerization and analysis of phase structure. *Cellulose*, *5*, 123–134.

Miyashita, Y., Suzuki, T., & Nishio, Y. (2002). Miscibility of cellulose acetate with vinyl polymers. *Cellulose*, *9*, 215–223.

Newman, S. P., & Jones, W. (1998). Synthesis, characterization and applications of layered double hydroxides containing organic guests. *New Journal of Chemistry*, *22*, 105–115.

Nishio, Y. (1994). Hyperfine composites of cellulose with synthetic polymers. In R. D. Gilbert (Ed.), *Cellulosic polymers, blends and composites* (pp. 95–113). Munich: Hanser.

Nishio, Y. (2006). Material functionalization of cellulose and related polysaccharides via diverse microcompositions. *Advances in Polymer Science*, *205*, 97–151.

Ohno, T., & Nishio, Y. (2006). Cellulose alkyl ester/vinyl polymer blends: Effects of butyryl substitution and intramolecular copolymer composition on the miscibility. *Cellulose*, *13*, 245–259.

Ohno, T., & Nishio, Y. (2007a). Estimation of miscibility and interaction for cellulose acetate and butyrate blends with *N*-vinylpyrrolidone copolymers. *Macromolecular Chemistry and Physics*, *208*, 622–634.

Ohno, T., & Nishio, Y. (2007b). Molecular orientation and optical anisotropy in drawn films of miscible blends composed of cellulose acetate and poly(*N*-vinylpyrrolidone-*co*-methyl methacrylate). *Macromolecules*, *40*, 3468–3476.

Ohno, T., Yoshizawa, S., Miyashita, Y., & Nishio, Y. (2005). Interaction and scale of mixing in cellulose acetate/poly(*N*-vinyl pyrrolidone-co-vinyl acetate) blends. *Cellulose*, *12*, 281–291.

Okada, A., Kawasumi, M., Usuki, A., Kojima, Y., Kurauchi, T., & Kamigaito, O. (1990). Nylon 6-clay hybrid. *Materials Research Society Symposium Proceedings*, *171*, 45–50.

O'Leary, S., O'Hare, D., & Seeley, G. (2002). Delamination of layered double hydroxides in polar monomers: New LDH-acrylate nanocomposites. *Chemical Communications*, *2002*, 1506–1507.

Park, H.-M., Misra, M., Drzal, L. T., & Mohanty, A. K. (2004). "Green" nanocomposites from cellulose acetate bioplastic and clay: Effect of eco-friendly triethyl citrate plasticizer. *Biomacromolecules*, *5*, 2281–2288.

Parrod, J., & Elles, J. (1958). Polyacrylamides dérivés d'amides cycliques. *Journal of Polymer Science*, *29*, 411–416.

Radloff, D., Boeffel, C., & Spiess, H. W. (1996). Cellulose and cellulose/poly(vinyl alcohol) blends. 2. Water organization revealed by solid-state NMR spectroscopy. *Macromolecules*, *29*, 1528–1534.

Spiegel, S., Schmidt-Rohr, K., Boeffel, C., & Spiess, H. W. (1993). ^{1}H spin diffusion coefficients of highly mobile polymers. *Polymer*, *34*, 4566–4569.

Utracki, L. A. (1990). *Polymer alloys and blends: Thermodynamics and rheology*. Munich: Hanser.

Whilton, N. T., Vickers, P. J., & Mann, S. (1997). Bioinorganic clays: Synthesis and characterization of amino- and polyamino acid intercalated layered double hydroxides. *Journal of Materials Chemistry*, *7*, 1623–1629.

Yano, K., Usuki, A., & Okada, A. (1997). Synthesis and properties of polyimide–clay hybrid films. *Journal of Polymer Science Part A: Polymer Chemistry*, *35*, 2289–2294.

Yoon, K.-B., Hwang, Y.-Y., Noh, S. K., & Lee, D.-H. (2008). Polymer nanocomposite of Mg–Al hydrotalcite-type anionic clay modified with organosulfate. *Polymer Journal*, *40*, 50–55.

Zhang, X., Takegoshi, K., & Hikichi, K. (1992). Composition dependence of the miscibility and phase structure of amorphous/crystalline polymer blends as studied by high-resolution solid-state ^{13}C NMR spectroscopy. *Macromolecules*, *25*, 2336–2340.